



Article

Model-Free Fractional-Order Sliding Mode Control of Electric Drive System Based on Nonlinear Disturbance Observer

Yingxin Yu ¹ and Xudong Liu ^{1,2,*} ¹ College of Automation, Qingdao University, Qingdao 266071, China² Shandong Key Laboratory of Industrial Control Technology, Qingdao 266071, China

* Correspondence: lxd2017@qdu.edu.cn

Abstract: A model-free fractional-order sliding mode control (MFFOSMC) method based on a non-linear disturbance observer is proposed for the electric drive system in this paper. Firstly, the ultra-local model is established by using the mathematical model of electric drive system under parameter perturbation. Then, aiming at reducing the chattering of the sliding mode controller and improving the transient response, a model-free fractional-order sliding mode controller is designed based on fractional-order theory. Next, considering that the traditional sliding mode control can only suppress matched disturbance and that it is sensitive to mismatched disturbance, a non-linear disturbance observer is used to estimate disturbance, and the estimated variables are used in the design of a sliding mode surface to improve the tracking accuracy of the system. Finally, the experiment is completed on an asynchronous motor drive platform. Compared with the model-free integer-order sliding mode control (MFIOSMC), the results show that the proposed method has good dynamic response and strong robustness. Meanwhile, the proposed method reduces the dependence on mathematical models.



Citation: Yu, Y.; Liu, X. Model-Free Fractional-Order Sliding Mode Control of Electric Drive System Based on Nonlinear Disturbance Observer. *Fractal Fract.* **2022**, *6*, 603.

<https://doi.org/10.3390/fractalfract6100603>

Academic Editors: Norbert Herencsar, Heng Liu, Aldo Jonathan Muñoz-Vázquez and Yongping Pan

Received: 29 August 2022

Accepted: 13 October 2022

Published: 16 October 2022

Publisher's Note: MDPI stays neutral with regard to jurisdictional claims in published maps and institutional affiliations.



Copyright: © 2022 by the authors. Licensee MDPI, Basel, Switzerland. This article is an open access article distributed under the terms and conditions of the Creative Commons Attribution (CC BY) license (<https://creativecommons.org/licenses/by/4.0/>).

Keywords: model-free fractional-order sliding mode control (MFFOSMC); electric drive system; non-linear disturbance observer (NDO); mismatched disturbance; asynchronous motor (AM)

1. Introduction

Due to reliable operation, simple structure and convenient maintenance, asynchronous motors (AMs) have been widely used in industrial and energy systems [1], such as electric vehicles [2], electric railway vehicles [3], and wind energy [4]. However, the drive and control system of the AMs is relatively complex, which limits the application in high-performance control. With the development of control theory and power electronic technology, the new control strategies of asynchronous motor have gained more attention. In these methods, the sliding mode control (SMC) has become a research hotspot due to the characteristics of simple structure and strong robustness to parameter perturbation and external disturbance [5]. However, the chattering of SMC is an inherent defect, which will affect control accuracy, damage running parts and increase energy consumption [6].

In recent studies, to suppress the chattering of sliding mode control, some scholars have combined sliding mode control technology with advanced control algorithms, such as neural network control [7], fuzzy control [8], and optimal control [9], but the controller becomes very complex. At the same time, the researchers curb the shortcomings of the sliding mode control through innovative algorithms. As a kind of high-order sliding mode control algorithm, the super-twisting sliding mode control algorithm can effectively weaken the chattering existing in the system, but it is also very complex [10]. Terminal sliding mode control can converge in finite time and reduce chattering, but it also suffers from singularity problems [11,12]. The improved reaching law method can directly act on the reaching process, which can effectively reduce the system chattering, but it is difficult to keep the system state on the sliding surface with zero error [13].

Considering the two deficiencies of sliding mode control: (1) The control system is not robust when the system is in the reaching stage. (2) The chattering phenomenon of the system after reaching the sliding mode surface, the integral sliding mode control (ISMC) [14] is established by adding an integral term to the sliding mode surface. ISMC can set the initial state of the system, so that the arrival phase of the system is eliminated to improve anti-disturbance performance [15]. Most of the existing studies about ISMC are based on integer-order method, but there is an overshoot problem [16]. Since the integer-order integral has an accumulative effect on the error, if the error between the initial signal and the given value is too large, the phenomenon of integral saturation will occur, which will lead to the large overshoot and the long adjustment time [17].

With the development of fractional-order theory, fractional calculus has received enormous attention in engineering control [18,19]. As a generalization of integer-order calculus, fractional-order differential can convert the sign function of control input into fractional-order derivative form, so that the chattering phenomenon caused by switch control action can be effectively avoided and high-precision control can be realized [17]. Fractional-order integral is a low-pass filter of a sign function that removes high-frequency components. In [20], the fractional-order terminal sliding mode control is introduced to integer-order non-linear systems, which reduces the chattering and improves the dynamic response of the system. Due to fractional-order tunability, the system can respond quickly and dynamically [21,22]. In [23], a discrete-time fractional-order terminal sliding mode control strategy is applied to linear motors. The control accuracy and response speed of the motor are improved, and it has certain robustness to uncertain disturbance. In [24], to ensure the system stability and simplify the design, a second-order sliding surface using a fractional module is constructed. For non-holonomic mobile robot system under external disturbances, fixed-time fractional-order global sliding mode control approach is proposed in [25] to against disturbances. A novel adaptive super-twisting non-linear fractional-order PID sliding mode control strategy using extended state observer is presented in [26], the results demonstrate that the proposed control strategy not only achieve good stability and dynamic properties, but also is robust to external disturbance. In order to improve the anti-disturbance performance of a bearingless induction motor control system, a fractional-order sliding mode control strategy based on improved load torque observer is proposed on the basis of the sliding mode speed regulation system in [27].

It should be noted that although the fractional-order sliding mode control algorithms have many advantages in motor control, it is still a model-based control method, besides the motor control performance is closely related to the model parameters. To reduce the dependence on mathematical models, a model-free adaptive control algorithm is proposed in [28]. In [29], the model-free sliding mode control is applied to PMSM, which simplifies the adjustment process of controller parameters. The experiment proves that the method has good robustness for the disturbance. A model-free non-singular terminal sliding mode control method is proposed in [30], which ensures that the PMSM can reliable operate regardless of permanent magnet demagnetization faults and external disturbance.

For unknown linear systems perturbed by odd-harmonics disturbances, a tracking control strategy that combine adaptive and repetitive control methods is presented in [31]. In [32], the digital design of adaptive repetitive control for a class of linear systems subject to time-varying periodic disturbance is proposed, whose periods are assumed to be identifiable. In [33], in order to further reduce the chattering caused by sliding mode control, the extended state observer is used to estimate the system disturbance, which improves the control accuracy of the system. The optimal double-layer sliding mode observer is proposed in [34], which can reduce chattering and improve tracking performances. The above algorithm has good robustness to the matched disturbance, and has limited effect on the mismatched disturbance. So as to suppress the disturbance of the mismatched term, the lumped disturbance is considered in the mathematical model [35], and the estimated value of the disturbance is used for feedforward compensation, which effectively suppresses the influence of the disturbance.

Motivated by the above analysis, a model-free fractional-order sliding mode control (MFFOSMC) method based on non-linear disturbance observer is proposed for asynchronous motor drive in this paper. First, the motor model is simplified to a ultra-local model, which reduces the complexity of model. Then, by introducing fractional calculus into the sliding mode surface, the chattering is reduced and the dynamic response of the system is improved. The lumped disturbance is estimated by using a non-linear disturbance observer, and the disturbance rejection performance of the system is further improved. The experimental results show that the proposed method has fast convergence performance and strong anti-disturbance performance.

The main contributions of this paper are summarized as follows.

- (1) The ultra-local model of the AM is established, which reduces the dependence on motor parameters.
- (2) A fractional-order sliding mode control method is proposed, which reduce the chattering of sliding mode control and improve dynamic performance. Speed-current no-cascade control structure is adopted to effectively simplify the system structure.
- (3) A model-free sliding-mode controller for asynchronous motors based on non-linear disturbance observer is designed, which not only improves the dynamic performance of the system, but also enhances the robustness of the system.

The remainder of this paper is arranged as follows. The Section 2 introduces the fractional-order calculus fundamental. The mathematical model and the ultra-local model of AM is established in Section 3. The MFFOSMC controller and the non-linear disturbance observer are designed in Section 4. The experimental results is shown in Section 5. A brief conclusions of the paper is presented in Section 6.

2. Fractional-Order Calculus Fundamentals

2.1. Introduction of Fractional-Order Calculus

Fractional-order operators are extensions of traditional integer-order calculus operators. Fractional-order calculus operators are defined as follows [36].

$${}_{t_0}D_t^\alpha f(t) = \begin{cases} \frac{d^\alpha}{dt^\alpha} f(t), \alpha > 0 \\ f(t), \alpha = 0 \\ \int f(\tau) d\tau^{-\alpha}, \alpha < 0 \end{cases} \quad (1)$$

where t_0 and t are the upper and lower bounds of the operator, α is the order of the calculus, $\alpha > 0$ is considered a differential, and $\alpha < 0$ is an integral.

During the development of fractional-order theory, scholars have given a variety of definitions, among which the R-L fractional integral of α -order is defined as [37,38]

$${}_{t_0}D_t^{-\alpha} f(t) = \frac{1}{\Gamma(\alpha)} \int_{t_0}^t (t - \tau)^{\alpha-1} f(\tau) dx \quad (2)$$

where $\alpha > 0$, $\Gamma(\alpha)$ is the Gamma function,

$$\Gamma(\alpha) = \int_0^\infty e^{-t} t^{\alpha-1} dt \quad (3)$$

The most common Caputo definition of α -order fractional-order calculus in the field of engineering control is

$${}_{t_0}^C D_t^\alpha f(t) = \frac{1}{\Gamma(n - \alpha)} \int_{t_0}^t (t - \tau)^{n-\alpha-1} f^{(n)}(\tau) dx \quad (4)$$

where $\alpha > 0$, $n > \alpha > n - 1$, $n \in N$.

The Laplace transform of α -order fractional-order calculus (0 initial condition) at $t = 0$ is

$$L\{D^\alpha f(t)\} = s^\alpha F(s) \tag{5}$$

2.2. Analysis of Fractional-Order Operators

The frequency domain analysis of the system can be carried out by bringing $s = j\omega$ into the transfer function.

In the frequency domain range (ω_b, ω_h) , the approximation order N is set, and the fractional-order operator can use the Oustaloup filter for a good approximation. When $1 > \alpha > 0$, the recursive filter of Oustaloup for s^α is

$$G_f(s) = K \prod_{k=-N}^N \frac{s + \omega'_k}{s + \omega_k} = s^\alpha \tag{6}$$

where ω'_k, ω_k, K are, respectively,

$$\omega'_k = \omega_b \left(\frac{\omega_h}{\omega_b}\right)^{\frac{k+N+1/2(1-\alpha)}{2N+1}}, \omega_k = \omega_b \left(\frac{\omega_h}{\omega_b}\right)^{\frac{k+N+1/2(1+\alpha)}{2N+1}}, K = \omega_h^\alpha \tag{7}$$

A modified oustaloup filter has been proposed in [39]. It is given by

$$s^\alpha = \left(\frac{d\omega_h}{b}\right)^\alpha \left(\frac{ds^2 + b\omega_h s}{d(1-\alpha)s^2 + b\omega_h s + d\alpha}\right) G_p \tag{8}$$

where ω'_k, ω_k, K are, respectively, $G_p(s) = \prod_{k=-N}^N \frac{s+\omega'_k}{s+\omega_k}, \omega'_k = \left(\frac{d\omega_b}{b}\right)^{\frac{-2k+\alpha}{2N+1}}, \omega_k = \left(\frac{b\omega_h}{a}\right)^{\frac{2k+\alpha}{2N+1}}, b = 10, d = 9.$

The fractional-order system is approximated by the Oustaloup filter.

2.3. Comparison of Fractional-Order Sliding Mode and Integer-Order Sliding Mode

Take a simple fractional-order linear sliding surface as an example for analysis [40]

$$s = {}_0D_t^r x(t) - Ax(t) \tag{9}$$

where $1 > r > 0, x \in R^n, A$ is the coefficient matrix and $A = (a_{ij}) \in R^{n \times n}.$

When the system state reaches the sliding mode surface, the fractional-order system and the integer-order system satisfy the following conditions

$${}_0D_t^r x(t) = Ax(t) \tag{10}$$

Solve Differential Equation (10)

$$x(t) = E_{r,1}(t)x_0 \tag{11}$$

where

$$E_{r,\beta}(t) = \sum_{k=0}^{\infty} \frac{A^k t^{rk}}{\Gamma(rk + \beta)}$$

is the state transfer function, β generally takes as $\beta = 1, \Gamma(\cdot)$ is the Gamma function, and it is defined in Equation (3).

The transfer function of the integer-order system is

$$E_{1,1}(t) = \sum_{k=0}^{\infty} \frac{A^k t^k}{\Gamma(k+1)} = \sum_{k=0}^{\infty} \frac{A^k t^k}{k!} = e^{At} \tag{12}$$

The transfer function of the fractional-order system is

$$E_{r,1}(t) = \sum_{k=0}^{\infty} \frac{A^k t^{rk}}{\Gamma(rk+1)} \approx \frac{1}{\Gamma(1-r)} A^{-1} t^{-r} \tag{13}$$

From (12) and (13), it can be obtained that the state variables of the integer-order system converge to zero at the speed of e^{At} on the sliding mode surface, and the state variables of the fractional-order system converge at the speed of t^{-r} . This indicates that the energy transfer of fractional-order sliding mode surfaces is slower than that of integer-order.

Figure 1 shows the comparison between fractional-order sliding mode control and integer-order sliding mode control. When the system state variable moves on the sliding surface, the switching control takes effect, and it takes time for the control output $u(t)$ to switch from $+u(t)$ to $-u(t)$. This process is called time delay. Time delay is the main cause of chattering. In Figure 1, when the system state reaches the sliding surface from the initial state (x_0, y_0) . For fractional-order systems, the switching control takes effect only when the system state reaches (x_1, y_1) , and the delay at this time is t_m . The system state will converge to zero in the form of t^{-r} . For an integer-order system, the switching control comes into play at (x_1', y_1') , where the delay is $t_{m'}$. The system state will converge to the origin in the form of e^{-t} . The delay time of the system depends on the actuator, so $t_m = t_{m'}$, that is, when $1 > r > 0$, $e^{-t_{m'}} > t_m^{-r}$. It can be seen from the above analysis that the chattering of the fractional-order system is smaller than that of the integer-order system, and the fractional-order system can effectively suppress the chattering added [39,40].

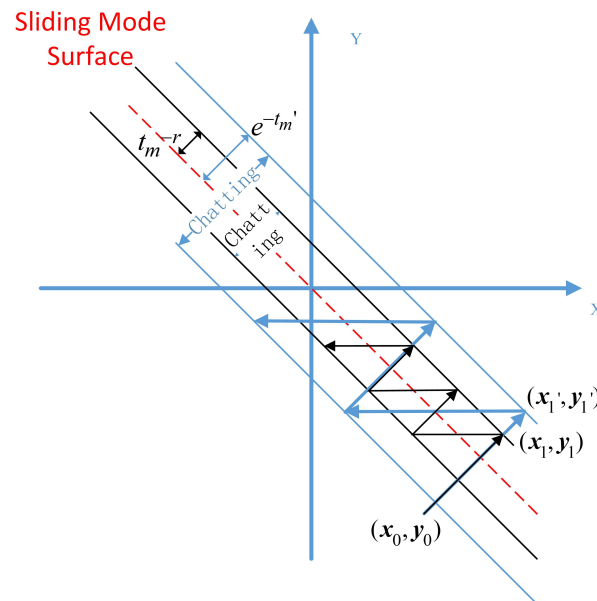


Figure 1. Comparison between fractional-order sliding mode control and integer-order sliding mode control.

3. Mathematical Model of AM

Based on the rotor field-oriented technology, the mathematical model of the AM in the d-q synchronous rotating frame can be expressed as

$$\begin{cases} \frac{di_{sd}}{dt} = \frac{u_{sd}}{L_c} - \left(\frac{R_s}{L_c} + \frac{L_m^2}{T_r L_c L_r} \right) i_{sd} + \omega_s i_{sq} + \frac{L_m}{T_r L_c L_r} \lambda_{rd} + f_{isd} \\ \frac{di_{sq}}{dt} = \frac{u_{sq}}{L_c} - \left(\frac{R_s}{L_c} + \frac{L_m^2}{T_r L_c L_r} \right) i_{sq} - \omega_s i_{sd} - \frac{L_m \omega_r}{L_c L_r} \lambda_{rd} + f_{isq} \\ \frac{d\lambda_{rd}}{dt} = \frac{1}{T_r} (L_m i_{sd} - \lambda_{rd}) + f_{\lambda} \\ \frac{d\omega}{dt} = \frac{1}{J} (T_e - T_L) + f_{\omega} \end{cases} \tag{14}$$

where $T_r = \frac{L_r}{R_r}$ represents the rotor time constant, $T_e = \frac{n_p L_m \lambda_{rd} i_{sq}}{R_r}$ is the electromagnetic torque, $\omega_r = n_p \omega$ denote rotor electrical angular velocity, $\omega_s = n_p \omega + \frac{L_m i_{sq}}{T_r \lambda_{rd}}$ denote stator electrical angular velocity, $L_c = \frac{L_s L_r - L_m^2}{L_r}$. n_p is the pole pairs, L_s , L_r , and L_m are the stator inductance, rotor inductance and mutual inductance, respectively. R_s and R_r are stator resistance and rotor resistance. U_{sd} and U_{sq} are the stator voltage of d-axis and q-axis. λ_{rd} , λ_{rq} represents the rotor flux of d-axis and q-axis, ω denote rotor mechanical angular velocity. J , T_L are the moment of inertia and load torque. f_{isd} , f_{isq} , f_λ , and f_ω are the lumped disturbances of motor system.

The second and fourth expressions in model (1) can be rewritten as

$$\begin{cases} \frac{di_{sq}}{dt} = \left(\frac{1}{L_c} - \alpha_1\right)u_{sq} + \alpha_1 u_{sq} - \left(\frac{R_s}{L_c} + \frac{L_m^2}{T_r L_c L_r}\right)i_{sq} - \omega_s i_{sd} - \frac{L_m \omega_r}{L_c L_r} \lambda_{rd} + f_{isq} \\ \frac{d\omega}{dt} = \left(\frac{1}{J} \frac{n_p L_m \lambda_{rd}}{L_r} - \alpha_2\right)i_{sq} + \alpha_2 i_{sq} - \frac{1}{J} T_L + f_\omega \end{cases} \tag{15}$$

where α_1, α_2 represent the proportional adjustable coefficient.

According to model-free theory [14], the model (15) can be simplified to a ultra-local model as

$$\begin{cases} \frac{di_{sq}}{dt} = \alpha_1 u_{sq} + F_{isq} \\ \frac{d\omega}{dt} = \alpha_2 i_{sq} + F_\omega \end{cases} \tag{16}$$

where $F_{isq} = \left(\frac{1}{L_c} - \alpha_1\right)u_{sq} - \left(\frac{R_s}{L_c} + \frac{L_m^2}{T_r L_c L_r}\right)i_{sq} - \omega_s i_{sd} - \frac{L_m \omega_r}{L_c L_r} \lambda_{rd} + f_{isq}$, $F_\omega = \left(\frac{1}{J} \frac{n_p L_m \lambda_{rd}}{L_r} - \alpha_2\right)i_{sq} - \frac{1}{J} T_L + f_\omega$ are the lumped disturbance including uncertain parameters and external unknown perturbation.

Define the speed error as

$$\omega_e = \omega^* - \omega \tag{17}$$

where ω^*, ω are the given speed and actual speed of motor.

By combining (16) and (17), the ultra-local model of the speed loop can be rewritten as

$$\begin{cases} (-\alpha_2) \frac{di_{sq}}{dt} = (-\alpha_2) \alpha_1 u_{sq} + (-\alpha_2) F_{isq} \\ \frac{d\omega_e}{dt} = \dot{\omega}^* - \dot{\omega} = \dot{\omega}^* - \alpha_2 i_{sq} - F_\omega \end{cases} \tag{18}$$

Let $x_1 = \omega_e, x_2 = -\alpha_2 i_{sq}$, then

$$\begin{cases} \dot{x}_2 = -\alpha_1 \alpha_2 u_{sq} + d_2 \\ \dot{x}_1 = x_2 + d_1 \end{cases} \tag{19}$$

where $d_1 = \dot{\omega}^* - F_\omega$, $d_2 = -\alpha_2 F_{isq}$. d_1 and d_2 are the mismatched disturbance and matched disturbance. Assuming that the system disturbance is bounded and slowly varying, the boundary of the disturbance can be expressed as $|d_1| \leq D_1, |\dot{d}_1| \leq D_{11}$ and $|d_2| \leq D_2, |\dot{d}_2| \leq D_{22}$, where D_1, D_{11}, D_2, D_{22} are positive.

4. Design of Speed Controller for AM

4.1. Analysis of Traditional Sliding Surface with Mismatched Terms

In the traditional sliding mode controller, the linear sliding mode surface is composed of state variables as follows

$$s = x_1 + c x_2 \tag{20}$$

where c is a constant and greater than 0.

Regardless of the system disturbance, when the system state reaches the sliding mode surface, the equivalent control of the system (19) is

$$u_{eq} = \frac{1}{c \alpha_1 \alpha_2} x_2 \tag{21}$$

The switching control of system (19) is

$$u_{sw} = \frac{k}{c\alpha_1\alpha_2} \text{sgn}(s) \quad (22)$$

where k is the designed controller gain, $k > 0$. Then, the designed controller is

$$u = u_{eq} + u_{sw} \quad (23)$$

Substitute the designed controller (23) into the sliding surface (20)

$$\dot{s} = d_1 + cd_2 - k\text{sgn}(s) \quad (24)$$

If the set value of k is greater than $d_1 + cd_2$, the system will eventually reach the sliding surface $s = 0$ [20]. On the sliding surface of the system and without considering the system chattering, it can be obtained

$$\dot{x}_1 = -\frac{1}{c}x_1 + d_1 \quad (25)$$

Solving the differential Equation (25)

$$x_1(t) = [x_1(0) - cd_1]e^{-t/c} + cd_1 \quad (26)$$

where $x_1(0)$ is the initial value of the system speed error variable.

From the analysis of Formula (26), when the system state reaches the sliding mode surface and $d_1 \neq 0$, the speed error variable $x_1(t)$ will not converge to 0. For the systems with mismatched disturbance, this is a problem faced by traditional sliding mode controllers.

4.2. Design of Fractional-Order Sliding Mode Controller

In order to obtain accurate and fast control of the motor speed, a novel fractional-order sliding mode surface with mismatched disturbance is designed as follows

$$s = c_{1t_0}D_t^{v-1}x_1 + c_2x_1 + x_2 + \hat{d}_1 \quad (27)$$

where $c_1 > 0$, $c_2 > 0$, $1 > v > 0$ are constants that need to be designed. The introduction of \hat{d}_1 is used to remove the effect of mismatched disturbance. Then, considering the advantages of the fractional-order relative to the integer-order, the dynamic performance of the system is improved by introducing the fractional-order term in the sliding mode surface.

The time derivative of sliding surface (27) is

$$\dot{s} = c_{1t_0}D_t^v x_1 + c_2(x_2 + d_1) - \alpha_1\alpha_2 u_{sq} + d_2 + \dot{\hat{d}}_1 \quad (28)$$

By introducing $s = 0$ into Equation (28), the equivalent controller of the system can be obtained as

$$u_{eq} = \frac{1}{\alpha_1\alpha_2} \left[c_{1t_0}D_t^v x_1 + c_2(x_1 + d_1) + d_2 + \dot{\hat{d}}_1 \right] \quad (29)$$

Using the exponential reaching law

$$\dot{s} = -\varepsilon\text{sgn}(s) - ks \quad (30)$$

The fractional-order sliding mode controller based on exponential reaching rate is designed as

$$\begin{aligned} u_{sq} &= u_{eq} + u_{sw} \\ &= \frac{1}{\alpha_1\alpha_2} \left[c_{1t_0}D_t^v x_1 + c_2(x_2 + d_1) + d_2 + \dot{\hat{d}}_1 \right] + \frac{1}{\alpha_1\alpha_2} [\varepsilon\text{sgn}(s) + ks] \end{aligned} \quad (31)$$

Define the Lyapunov function as [40,41]

$$V = \frac{1}{2}s^2 \tag{32}$$

Then

$$\begin{aligned} \dot{V} &= s\dot{s} \\ &= s \left[c_{1t_0} D_t^\nu x_1 + c_2(x_2 + d_1) - \alpha_1\alpha_2 u_{sq} + d_2 + \hat{d}_1 \right] \\ &= s \left[c_{1t_0} D_t^\nu x_1 + c_2(x_2 + d_1) - \alpha_1\alpha_2 \left\{ \frac{1}{\alpha_1\alpha_2} \left[c_{1t_0} D_t^\nu x_1 + c_2(x_2 + d_1) + d_2 + \hat{d}_1 \right] \right. \right. \\ &\quad \left. \left. + \frac{1}{\alpha_1\alpha_2} [\varepsilon \operatorname{sgn}(s) + ks] \right\} + d_2 + \hat{d}_1 \right] \\ &= -\varepsilon|s| - ks^2 \end{aligned} \tag{33}$$

When the parameters satisfy conditions of $\varepsilon > 0, k > 0$, then $\dot{V} \leq 0$ is satisfied. According to Lyapunov stability theory, the designed controller is asymptotically stable.

To sum up, the diagram of the composite control system of AM based on MFFSMC is shown in Figure 2. The composite control system consists of flux linkage regulator, speed regulator, vector coordinate transformation module, space vector pulse width modulation module, converter module, asynchronous motor, flux linkage observer, and non-linear disturbance observer, where the flux linkage regulator is a cascaded PI controller, speed regulator is the designed MFFOSMC controller.

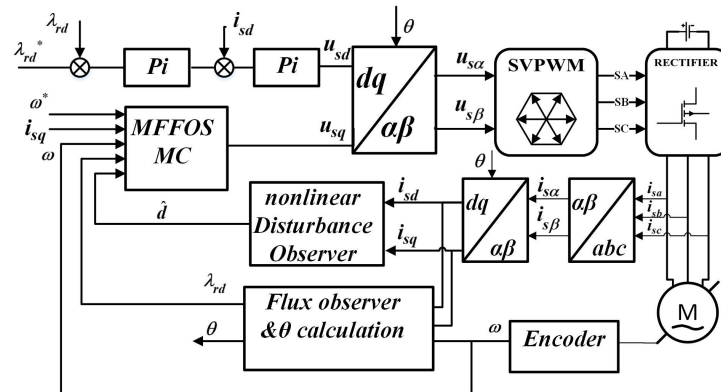


Figure 2. The diagram of the composite control system of AM based on MFFSMC.

4.3. Design of Non-linear Disturbance Observer

Since the system performance is affected by the uncertainty of the motor parameters and the load disturbance, in order to improve the anti-disturbance performance of the fractional-order sliding mode controller and the dynamic response of the system, a non-linear disturbance observer is constructed. By compensating the estimated disturbance to the single-loop controller, the influence of disturbance on the system is reduced.

Converting the ultra-local model (19) into matrix form

$$\begin{bmatrix} \dot{x}_1 \\ \dot{x}_2 \end{bmatrix} = \begin{bmatrix} 0 & 1 \\ 0 & 0 \end{bmatrix} \begin{bmatrix} x_1 \\ x_2 \end{bmatrix} + \begin{bmatrix} 0 \\ -\alpha_1\alpha_2 \end{bmatrix} u_{sq} + \begin{bmatrix} 1 & 0 \\ 0 & 1 \end{bmatrix} \begin{bmatrix} d_1 \\ d_2 \end{bmatrix} \tag{34}$$

The estimated values of d_1 and d_2 are written as

$$\begin{bmatrix} \hat{d}_1 \\ \hat{d}_2 \end{bmatrix} = \begin{bmatrix} p_1 \\ p_2 \end{bmatrix} + \begin{bmatrix} r_1 & 0 \\ 0 & r_2 \end{bmatrix} \begin{bmatrix} x_1 \\ x_2 \end{bmatrix} \tag{35}$$

where p_1, p_2 are intermediate variables and r_1, r_2 are observer gains.

Substituting (35) into (34), then

$$\begin{cases} \begin{bmatrix} \dot{p}_1 \\ \dot{p}_2 \end{bmatrix} = - \begin{bmatrix} r_1 & 0 \\ 0 & r_2 \end{bmatrix} \begin{bmatrix} \dot{x}_1 \\ \dot{x}_2 \end{bmatrix} \\ = - \begin{bmatrix} r_1 & 0 \\ 0 & r_2 \end{bmatrix} \left\langle \begin{bmatrix} 0 & 1 \\ 0 & 0 \end{bmatrix} \begin{bmatrix} x_1 \\ x_2 \end{bmatrix} + \begin{bmatrix} 0 \\ -\alpha_1\alpha_2 \end{bmatrix} u_{sq} + \begin{bmatrix} 1 & 0 \\ 0 & 1 \end{bmatrix} \left\{ \begin{bmatrix} p_1 \\ p_2 \end{bmatrix} + \begin{bmatrix} r_1 & 0 \\ 0 & r_2 \end{bmatrix} \begin{bmatrix} x_1 \\ x_2 \end{bmatrix} \right\} \right\rangle \\ \begin{bmatrix} \hat{d}_1 \\ \hat{d}_2 \end{bmatrix} = \begin{bmatrix} p_1 \\ p_2 \end{bmatrix} + \begin{bmatrix} r_1 & 0 \\ 0 & r_2 \end{bmatrix} \begin{bmatrix} x_1 \\ x_2 \end{bmatrix} \end{cases} \quad (36)$$

The structure of the non-linear disturbance observer designed in this section is shown in Figure 3.

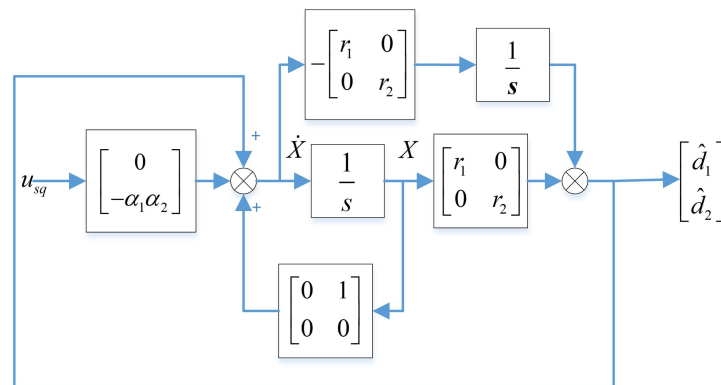


Figure 3. The structure of the non-linear disturbance observer.

5. Experimental Results

In order to validate the effectiveness of the proposed model-free fractional-order sliding mode control with non-linear disturbance observer for AM, the experiment is completed based on a hardware-in-loop experimental platform LINKS-RT. The photograph of experimental platform is shown in Figure 4. Table 1 lists the parameters of the AM.

To demonstrate the superiority of the proposed method, the speed controllers based on MFFOSMC and MFIOSMC with disturbance observer are designed for comparison. The parameters of control system are obtained by trial and error method. The parameters of model-free fractional-order sliding mode controller are chosen as $k = 5$, $v = 0.8$, $c_1 = 1200$, $c_2 = 5$, and $\epsilon = 5$.

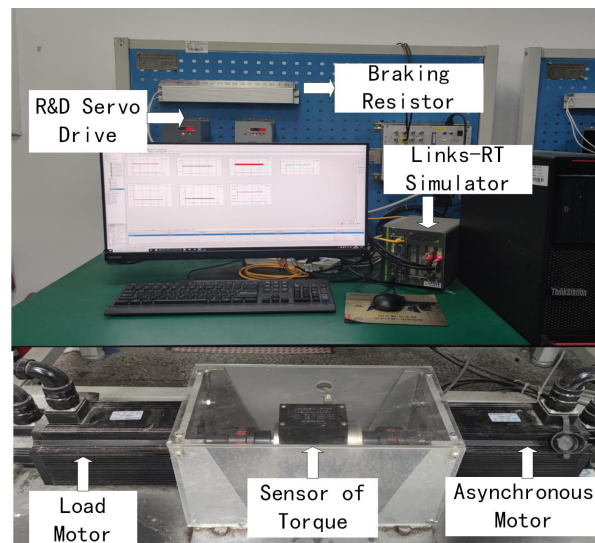


Figure 4. Experimental platform.

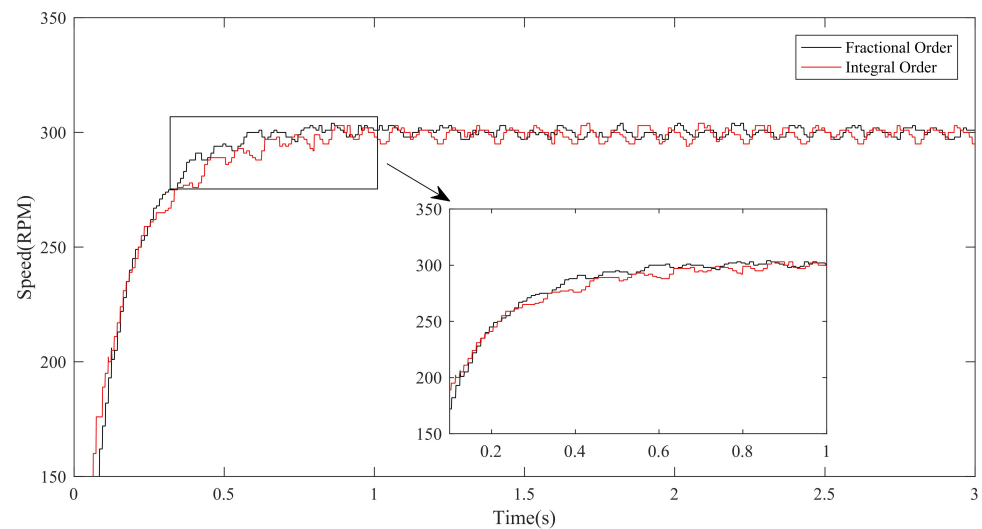
Table 1. Parameters of AM.

Parameters	Symbol	Value
rated power	P_N	1.5 KW
rated stator voltage	U_N	220 V
rated stator current	I_N	5.9 A
stator resistance	R_s	0.96 Ω
rotor resistance	R_r	0.93 Ω
stator inductance	L_s	118.32 mH
rotor inductance	L_r	118.67 mH
mutual inductance	L_m	112.23 mH
number of pole pairs	n_p	2
moment of inertia	J	0.0038 kg·m ²

5.1. Low Speed Performance

5.1.1. Low Speed Startup Performance

Firstly, the transient response experiments of the proposed method are performed under low reference speed. The reference speed is given as $n = 300$ r/min, and the results are shown in Figure 5. It can be seen from Figure 5 that the setting times are 0.8 s and 0.9 s, based on MFOSMC + NDO and MFIOSMC + NDO, respectively. As shown in Figure 6, the speed fluctuations under MFIOSMC + NDO is 11 r/min, the proposed method reduce speed fluctuation by 27% (3 r/min). Compared with MFIOSMC + NDO, the proposed MFOSMC + NDO has the shortest setting time and smaller speed fluctuation under low reference speed.

**Figure 5.** The response curves at low speed.

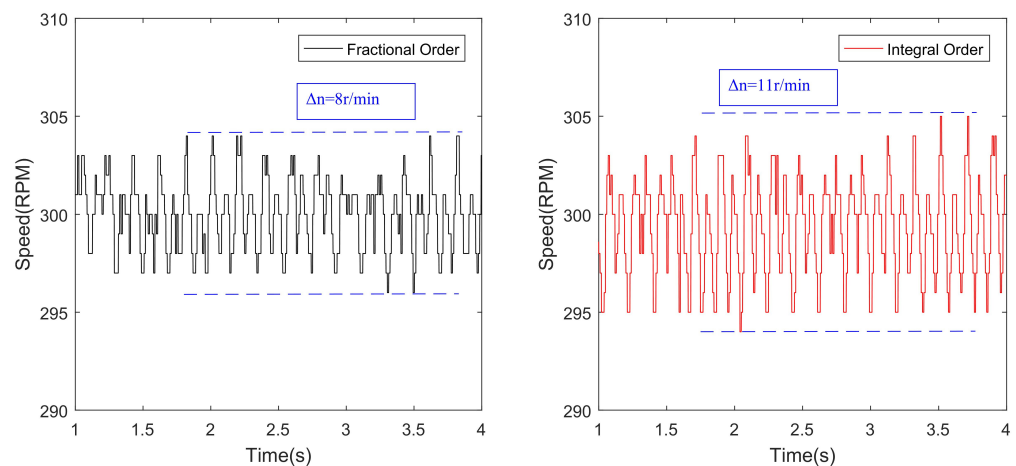


Figure 6. The speed fluctuation of motor at low speed.

5.1.2. Low Speed Anti-Disturbance Performance

To further verify the robustness for external disturbance, the anti-disturbance experiment is provided. In order to test this performance, when the motor is running at 300 r/min, the load torque of 3.5 N·m is suddenly added to the motor at $t = 5$ s and removed at $t = 10$ s. The anti-disturbance curve of 300r/min speed is shown in Figure 7. Figure 7 illustrates that the steady-state speed of the fractional-order sliding mode controller fluctuates to 265 r/min when the load torque is added in 5 s, and returns to the set speed at 5.6 s; the steady-state speed of the integer-order sliding mode controller fluctuates to 258 r/min, and reaches the set speed at 5.8 s. When the load torque is canceled within 10 s, the speed of the integer-order sliding mode controller fluctuates to 338 r/min, and resumes the set speed at 10.8 s; the speed of the fractional-order sliding mode controller fluctuates to 332 r/min, and reaches the set speed at 10.8 s. The results prove that the fractional-order sliding mode controller can better reduce the impact of disturbance, increase the robustness of the system.

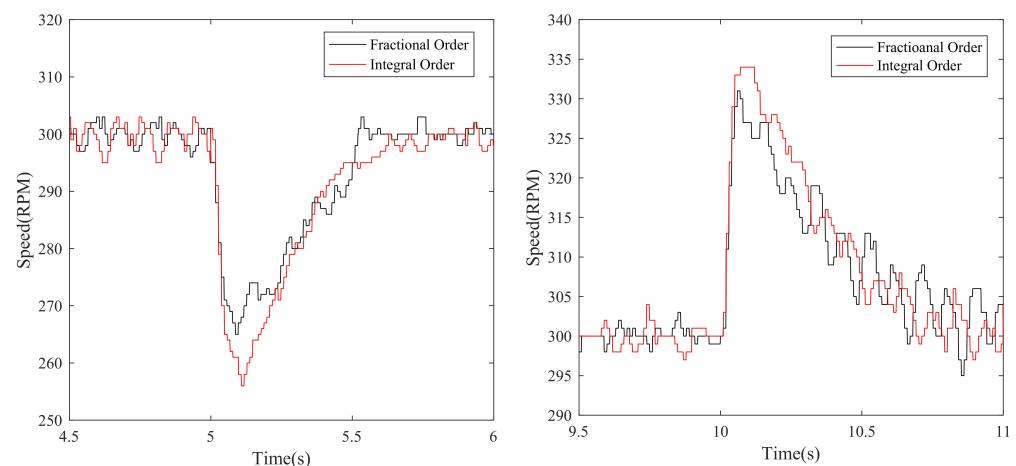


Figure 7. The speed curves with disturbance at low speed.

5.2. Middle Speed Performance

5.2.1. Middle Speed Startup Performance

Then, the startup control performance of the methods MFOSMC + NDO and MFIOSMC + NDO under middle reference speed are compared. The experimental results are shown in Figures 8 and 9. It can be seen from Figure 8 that the settling time using the method MFIOSMC + NDO to reference speed is 0.85 s, while the settling time using the method MFOSMC + NDO to reference speed is 0.75 s. From Figure 9, we can see that the speed

fluctuation is about 8 r/min, 12 r/min, respectively. The result above show that the proposed MFFOSMC + NDO has the faster dynamic response time and less chattering.

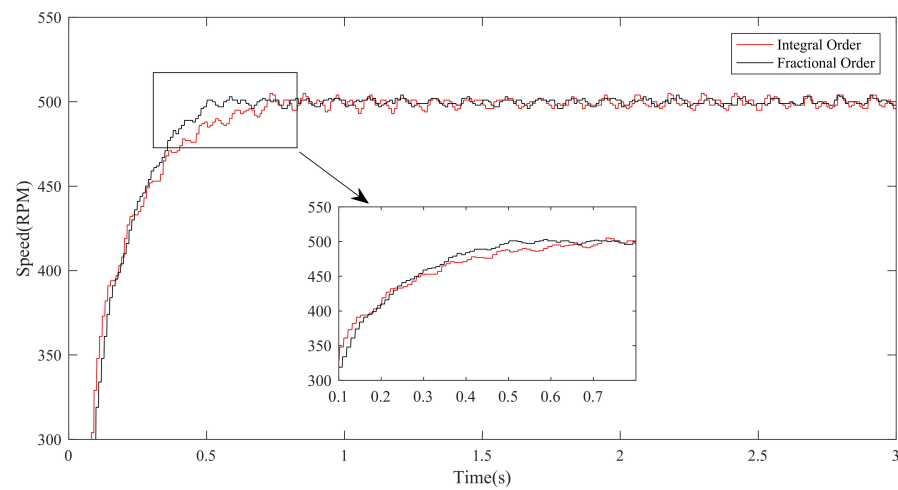


Figure 8. The response curves at middle speed.

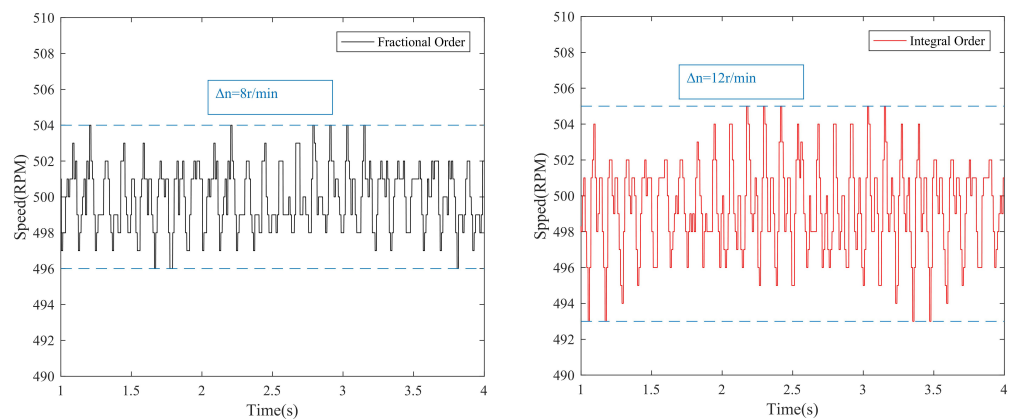


Figure 9. The speed fluctuation of motor at middle speed.

5.2.2. Middle Speed Anti-Disturbance Performance

In this experiment, we test the speed fluctuation due to external disturbance. The test conditions are that the motor runs in 500 r/min, and a load torque of 3.5 N·m is added at $t = 5$ s and then removed at $t = 10$ s. The anti-disturbance curve of 500 r/min speed is shown in Figure 10. The waveforms illustrates that the steady-state speed with the fractional-order sliding mode controller fluctuates to 465 r/min when the load torque is added in 5 s, and returns to the set speed at 5.6 s. The steady-state speed with the integer-order sliding mode controller fluctuates to 460 r/min, and reaches the set speed at 5.8 s. When the load disturbance is removed at $t = 10$ s, the motor speed of the integer-order sliding mode controller rises to 532 r/min and the motor speed of the fractional-order sliding mode controller rises to 530 r/min. The recovery time is about 0.8 s. As seen in Figure 10, when the load torque is changed, the proposed method under middle speed has the smaller speed fluctuation.

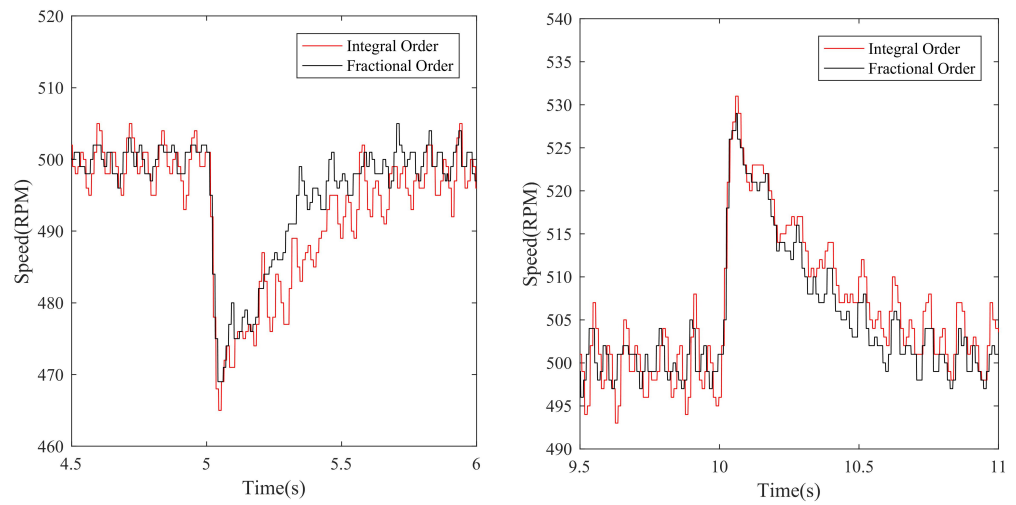


Figure 10. The speed curves with disturbance at middle speed.

5.3. High Speed Performance

5.3.1. High Speed Startup Performance

Finally, the control performance of the proposed method under high reference speed is tested, and the experimental results are shown in Figures 11 and 12. Figure 11 shows that based on two methods is 0.82 s and 0.9 s, respectively. Figure 12 indicates that the steady-state speed fluctuation with the fractional-order sliding mode controller is 10 r/min, while the steady-state speed fluctuation with the integer-order sliding mode controller is 12 r/min. According to the above analyses, the proposed MFOSMC + NDO has the better transient performance and the smaller speed fluctuation.

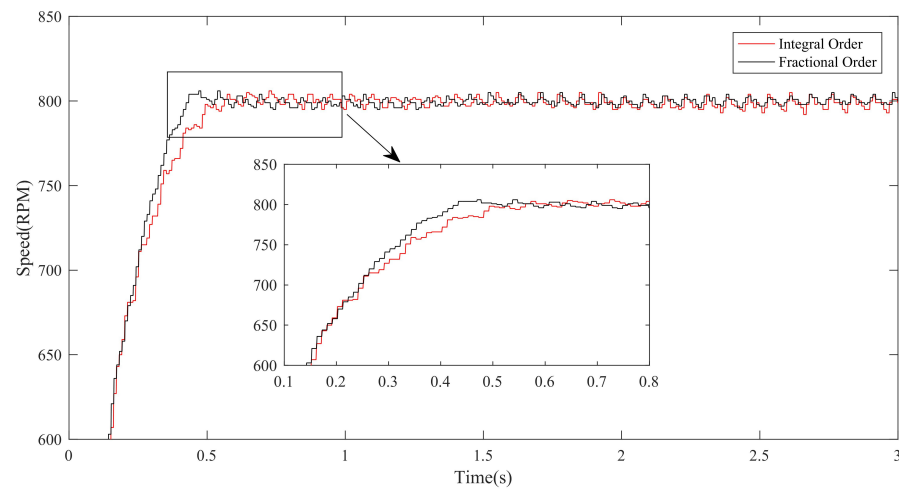


Figure 11. The response curves at high speed.

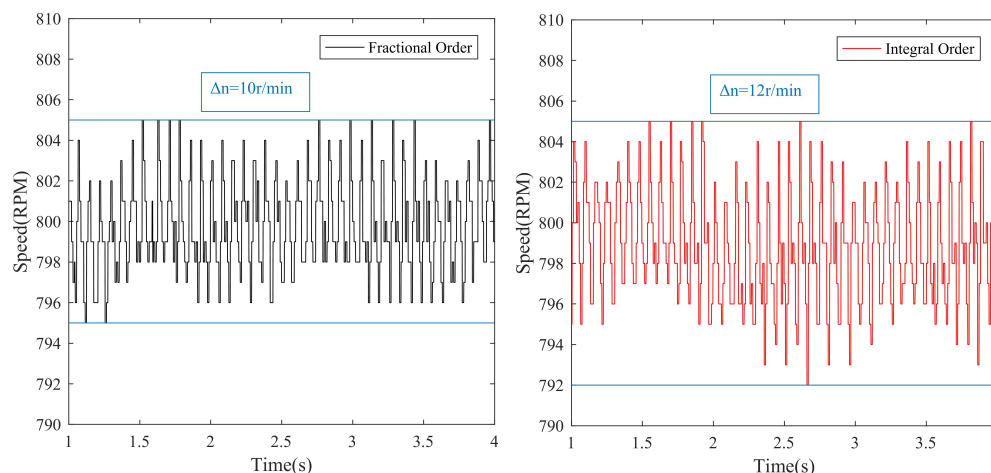


Figure 12. The speed fluctuation of motor at high speed.

5.3.2. High Speed Anti-Disturbance Performance

The robustness performance for the disturbance under high speed is very important. To validate the superiority of the proposed approach, when the motor is running at 800 r/min, the load torque of 3.5 N·m is added to the motor at $t = 5$ s and removed at $t = 10$ s. The results are shown in Figure 13. It is obvious from Figure 13 that when the load torque is added in 5 s, the speed with the integer-order sliding mode controller fluctuates to 763 r/min, and returns to the set speed at 5.8 s; the speed with fractional-order sliding mode controller fluctuates to 775 r/min, and reaches the set speed again at 5.5 s. When the load torque is canceled at 10s, the speed with the integer-order sliding mode controller fluctuates to 835 r/min, and resumes to the set speed at 10.8 s. The speed with fractional-order sliding mode controller fluctuates to 828 r/min, and reaches the set speed at 10.8 s. The results above show that the proposed method under high speed has the strong robustness.

In order to show the operation of asynchronous motor clearly, the detailed comparison of the two control algorithms at different speeds are summarized in Table 2. It can be seen from the Table 2 that the proposed method has smaller mean square error and achieves better speed tracking control. The experimental results above show that the proposed control strategy with MFFOSMC + NDO has the fast convergence speed, the good steady performance and the strong robustness for disturbance.

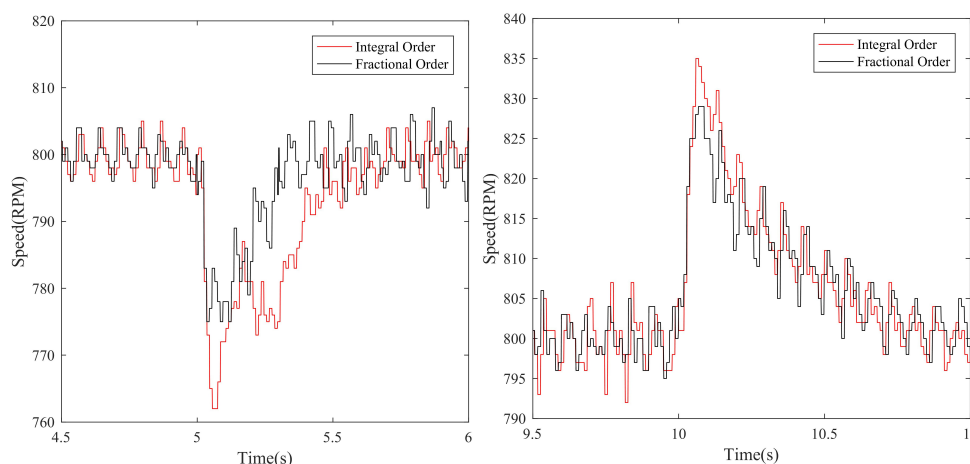


Figure 13. The speed curves with disturbance at high speed.

Table 2. Detailed comparison of the two control algorithms at different speeds.

Speed	Control Scheme	Root Mean Square Error
300 rpm	MFIOSMC	4.2948
300 rpm	MFFOSMC	4.2795
500 rpm	MFIOSMC	5.6966
500 rpm	MFFOSMC	5.5471
800 rpm	MFIOSMC	7.2379
800 rpm	MFFOSMC	7.1444

6. Conclusions

Aiming at the speed regulation problem of an asynchronous motor, a model-free fractional-order sliding mode controller based on non-linear disturbance observer is proposed in this paper. Mismatched disturbance are introduced in the sliding mode surface and estimated by the non-linear disturbance observer to eliminate the influence of non-linear disturbance. At the same time, due to the effect of fractional-order sliding mode surface, the dynamic performance of the system is improved and the robustness of the system is enhanced. The experimental results show that compared with the traditional integer-order sliding mode controller, the proposed control strategy has faster response time, better tracking performance, and stronger anti-disturbance ability at different speeds.

Author Contributions: Conceptualization, X.L. and Y.Y.; methodology, Y.Y.; software, Y.Y.; validation, X.L.; formal analysis, Y.Y.; investigation, Y.Y.; resources, X.L.; data curation, X.L.; writing—original draft preparation, Y.Y.; writing—review and editing, Y.Y.; visualization, X.L.; supervision, X.L.; project administration, X.L.; funding acquisition, X.L. All authors have read and agreed to the published version of the manuscript.

Funding: This research was funded by the National Natural Science Foundation of China under Grant No. 52037005, in part by the China Postdoctoral Science Foundation under Grant No. 2018M632622, in part by the Science and Technology Support Plan for Youth Innovation of Universities in Shandong Province under Grant No. 2019KJN033.

Conflicts of Interest: The authors declare no conflict of interest.

Abbreviations

The following abbreviations are used in this manuscript:

MFFOSMC	Model-free fractional-order sliding mode control
MFIOSMC	Model-free integer-order sliding mode control
AM	Asynchronous motors
NDO	Non-linear disturbance observer
SMC	Sliding mode control
ISMC	Integral sliding mode control

References

- Quintero-Manriquez, E.; Sanchez, E.N.; Antonio-Toledo, M.E.; Munoz, F. Neural control of an induction motor with regenerative braking as electric vehicle architecture. *Eng. Appl. Artif. Intell.* **2021**, *104*, 104275. [[CrossRef](#)]
- Mohanraj, D.; Gopalakrishnan, J.; Chokkalingam, B.; Mihet-Popa, L. Critical Aspects of Electric Motor Drive Controllers and Mitigation of Torque Ripple-Review. *IEEE Access* **2022**, *10*, 73635–73674. [[CrossRef](#)]
- Nagataki, M.; Kondo, K.; Yamazaki, O.; Yuki, K.; Nakazawa, Y. Online Auto-Tuning Method in Field-Orientation-Controlled Induction Motor Driving Inertial Load. *IEEE Open J. Ind. Appl.* **2022**, *3*, 125–140. [[CrossRef](#)]
- Dias, F.J.M.; Sotelo, G.G.; de Andrade Júnior, R. Performance Comparison of Superconducting Machines With Induction Motors. *IEEE Trans. Appl. Supercond.* **2022**, *32*, 1–5. [[CrossRef](#)]
- Song, S.; Meng, B.; Wang, Z. On Sliding Mode Control for Singular Fractional-Order Systems with Matched External Disturbances. *Fractal Fract.* **2022**, *6*, 366. [[CrossRef](#)]
- Shi, D.; Zhang, J.; Sun, Z.; Xia, Y. Adaptive sliding mode disturbance observer-based composite trajectory tracking control for robot manipulator with prescribed performance. *Nonlinear Dyn.* **2022**, *109*, 2693–2704. [[CrossRef](#)]

7. Sacchi, N.; Incremona, G.P.; Ferrara, A. Neural Network-Based Practical/Ideal Integral Sliding Mode Control. *IEEE Control Syst. Lett.* **2022**, *6*, 3140–3145. [[CrossRef](#)]
8. Lin, H.; Liu, J.; Shen, X.; Leon, J.I.; Vazquez, S.; Alcaide, A.M.; Wu, L.; Franquelo, L.G. Fuzzy Sliding-Mode Control for Three-Level NPC AFE Rectifiers: A Chattering Alleviation Approach. *IEEE Trans. Power Electron.* **2022**, *37*, 11704–11715. [[CrossRef](#)]
9. Yuan, L.; Li, J. Consensus of Discrete-Time Nonlinear Multiagent Systems Using Sliding Mode Control Based on Optimal Control. *IEEE Access* **2022**, *10*, 47275–47283. [[CrossRef](#)]
10. Fei, J.; Feng, Z. Fractional-Order Finite-Time Super-Twisting Sliding Mode Control of Micro Gyroscope Based on Double-Loop Fuzzy Neural Network. *IEEE Trans. Syst.* **2021**, *51*, 7692–7706. [[CrossRef](#)]
11. Dong, H.; Yang, X.; Gao, H.; Yu, X. Practical Terminal Sliding-Mode Control and Its Applications in Servo Systems. *IEEE Trans. Ind. Electron.* **2023**, *70*, 752–761. [[CrossRef](#)]
12. Hou, H.; Yu, X.; Xu, L.; Rsetam, K.; Cao, Z. Finite-Time Continuous Terminal Sliding Mode Control of Servo Motor Systems. *IEEE Trans. Ind. Electron.* **2020**, *67*, 5647–5656. [[CrossRef](#)]
13. Sun, X.; Cao, J.; Lei, G.; Guo, Y.; Zhu, J. A Composite Sliding Mode Control for SPMSM Drives Based on a New Hybrid Reaching Law With Disturbance Compensation. *IEEE Trans. Transp. Electrification* **2021**, *7*, 1427–1436. [[CrossRef](#)]
14. Li, T.; Liu, X. Model-Free Non-Cascade Integral Sliding Mode Control of Permanent Magnet Synchronous Motor Drive with a Fast Reaching Law. *Symmetry* **2021**, *13*, 1680. [[CrossRef](#)]
15. Xu, Y.; Li, S.; Zou, J. Integral Sliding Mode Control Based Deadbeat Predictive Current Control for PMSM Drives with Disturbance Rejection. *IEEE Trans. Power Electron.* **2022**, *37*, 2845–2856. [[CrossRef](#)]
16. Pan, Y.; Yang, C.; Pan, L.; Yu, H. Integral Sliding Mode Control: Performance, Modification, and Improvement. *IEEE Trans. Ind. Inform.* **2018**, *14*, 3087–3096. [[CrossRef](#)]
17. Huang, S.; Xiong, L.; Wang, J.; Li, P.; Wang, Z.; Ma, M. Fixed-Time Fractional-Order Sliding Mode Controller for Multimachine Power Systems. *IEEE Trans. Power Syst.* **2021**, *36*, 2866–2876. [[CrossRef](#)]
18. Wang, B.; Wang, S.; Peng, Y.; Pi, Y.; Luo, Y. Design and High-Order Precision Numerical Implementation of Fractional-Order PI Controller for PMSM Speed System Based on FPGA. *Fractal Fract.* **2022**, *6*, 218. [[CrossRef](#)]
19. Zheng, W.; Huang, R.; Luo, Y.; Chen, Y.; Wang, X.; Chen, Y. A Look-Up Table Based Fractional Order Composite Controller Synthesis Method for the PMSM Speed Servo System. *Fractal Fract.* **2022**, *6*, 47. [[CrossRef](#)]
20. Babes, B.; Mekhilef, S.; Boutaghane, A.; Rahmani, L. Fuzzy Approximation-Based Fractional-Order Nonsingular Terminal Sliding Mode Controller for DC–DC Buck Converters. *IEEE Trans. Power Electron.* **2022**, *37*, 2749–2760. [[CrossRef](#)]
21. Efe, M.Ö. Fractional Order Systems in Industrial Automation—A Survey. *IEEE Trans. Ind. Inform.* **2011**, *7*, 582–591. [[CrossRef](#)]
22. Xu, S.; Sun, G.; Ma, Z.; Li, X. Fractional-Order Fuzzy Sliding Mode Control for the Deployment of Tethered Satellite System Under Input Saturation. *IEEE Trans. Aerosp. Electron. Syst.* **2019**, *55*, 747–756. [[CrossRef](#)]
23. Sun, G.; Ma, Z.; Yu, J. Discrete-Time Fractional Order Terminal Sliding Mode Tracking Control for Linear Motor. *IEEE Trans. Ind. Electron.* **2018**, *65*, 3386–3394. [[CrossRef](#)]
24. Labbadi, M.; Boubaker, S.; Djemai, M.; Mekni, S.K.; Bekrar, A. Fixed-Time Fractional-Order Global Sliding Mode Control for Nonholonomic Mobile Robot Systems under External Disturbances. *Fractal Fract.* **2022**, *6*, 177. [[CrossRef](#)]
25. Fang, Y.; Li, S.; Fei, J. Adaptive Intelligent High-Order Sliding Mode Fractional Order Control for Harmonic Suppression. *Fractal Fract.* **2022**, *6*, 1756–1765. [[CrossRef](#)]
26. Gao, P.; Zhang, G.; Ouyang, H.; Mei, L. An Adaptive Super Twisting Nonlinear Fractional Order PID Sliding Mode Control of Permanent Magnet Synchronous Motor Speed Regulation System Based on Extended State Observer. *IEEE Access* **2020**, *8*, 53498–53510. [[CrossRef](#)]
27. Yang, Z.; Ding, Q.; Sun, X.; Zhu, H.; Lu, C. Fractional-order sliding mode control for a bearingless induction motor based on improved load torque observer. *J. Frankl. Inst.* **2021**, *358*, 3701–3725. [[CrossRef](#)]
28. Hou, Z.; Xiong, S. On Model-Free Adaptive Control and Its Stability Analysis. *IEEE Trans. Autom. Control* **2019**, *64*, 4555–4569. [[CrossRef](#)]
29. Zhao, Y.; Liu, X.; Yu, H.; Yu, J. Model-free adaptive discrete-time integral terminal sliding mode control for PMSM drive system with disturbance observer. *IET Electr. Power Appl.* **2020**, *14*, 1756–1765. [[CrossRef](#)]
30. Zhao, K.; Yin, T.; Zhang, C.; He, J.; Li, X.; Chen, Y.; Zhou, R.; Leng, A. Robust Model-Free Nonsingular Terminal Sliding Mode Control for PMSM Demagnetization Fault. *IEEE Access* **2019**, *7*, 15737–15748. [[CrossRef](#)]
31. Kurniawan, E.; Harno, H.G.; Wang, H.; Prakosa, J.A.; Sirenden, B.H.; Septanto, H.; Adinanta, H.; Rahmatillah, A. Robust adaptive repetitive control for unknown linear systems with odd-harmonics periodic disturbances. *SCIENCE CHINA Inf. Sci.* **2022**, *1*.
32. Kurniawan, E.; Cao, Z.; Man, Z. Digital design of adaptive repetitive control of linear systems with time-varying periodic disturbances. *IET Control Theory Appl.* **2014**, *8*, 1995–2003. [[CrossRef](#)]
33. Zhang, Y.; Jin, J.; Huang, L. Model-Free Predictive Current Control of PMSM Drives Based on Extended State Observer Using Ultralocal Model. *IEEE Trans. Ind. Electron.* **2021**, *68*, 993–1003. [[CrossRef](#)]
34. Zhou, J.; Tian, D.; Sheng, Z.; Duan, X.; Qu, G.; Cao, D.; Shen, X. Decentralized Robust Control for Vehicle Platooning Subject to Uncertain Disturbances via Super-Twisting Second-Order Sliding-Mode Observer Technique. *IEEE Trans. Veh. Technol.* **2022**, *71*, 7186–7201. [[CrossRef](#)]
35. Liu, X.; Yu, H. Continuous adaptive integral-type sliding mode control based on disturbance observer for PMSM drives. *Nonlinear Dyn.* **2021**, *104*, 1429–1441. [[CrossRef](#)]

36. Jafarlou, F.; Peimani, M.; Lotfivand, N. Fractional order adaptive sliding-mode finite time control for cable-suspended parallel robots with unknown dynamics. *Int. J. Dyn. Control* **2022**, *10*, 1674–1684. [[CrossRef](#)]
37. Aghababa, M.P. A Lyapunov-based control scheme for robust stabilization of fractional chaotic systems. *Nonlinear Dyn.* **2014**, *78*, 2129–2140. [[CrossRef](#)]
38. Ullah, N.; Ali, M.A.; Ibeas, A.; Herrera, J. Adaptive Fractional Order Terminal Sliding Mode Control of a Doubly Fed Induction Generator-Based Wind Energy System. *IEEE Access* **2017**, *5*, 21368–21381. [[CrossRef](#)]
39. Gu, G. Linear Feedback Control—Analysis and Design with MATLAB. *IEEE Control Syst. Mag.* **2009**, *29*, 128–129.
40. Zhang, B.; Pi, Y.; Luo, Y. Fractional order sliding-mode control based on parameters auto-tuning for velocity control of permanent magnet synchronous motor. *ISA Trans.* **2012**, *51*, 649–656. [[CrossRef](#)]
41. Long, B.; Lu, P.J.; Chong, K.T.; Rodriguez, J.; Guerrero, J.M. Robust Fuzzy-Fractional-Order Nonsingular Terminal Sliding-Mode Control of LCL-Type Grid-Connected Converters. *IEEE Trans. Ind. Electron.* **2022**, *69*, 5854–5866. [[CrossRef](#)]